E3S Web of Conferences **397**, 01003 (2023) https://doi.org/10.1051/e3sconf/202339701003
Mathematical Models and Methods of the Analysis and Optimal Synthesis of the Developing Pipeline and Hydraulic Systems 2022

An experimental investigation of the stochastic nature of slug flow

César García[1], *Leonid* Korelstein[2,*], *Carina* N. Sondermann[1], and *Eduardo* Pereyra[1]

[1]McDougall School of Petroleum Engineering, The University of Tulsa, Tulsa, OK, United States
[2]Piping Systems Research & Engineering Co, 7 Plekhanova Street, Moscow

Abstract. Slug flow is widely encountered in oil and gas systems. It has an unsteady hydrodynamic behavior that motivated the development of mechanistic models to better understand and quantify the parameters of the flow. The present work investigated several slug flow conditions through an experimental campaign that was performed in a 2-in ID horizontal pipe facility. The experimental data were statistically analyzed and they indicated the suitability of a lognormal distribution to model the flow characteristics, such as slug length, film length, and frequency. Based on the mean results, slug and film lengths tend to increase as more gas is present in the flow. The mean frequency indicated that higher frequencies are obtained with lower gas fractions. All the slugs from each test were individually studied using different approaches to analyze the data. The results suggest the existence of a relationship between the slug and film lengths when the slug unit is identified starting from a film region followed by a slug region. The values of the coefficient of determination for the relation between slug length and film length indicate a possible influence of other flow parameters of stochastic nature, such as slug liquid holdup, that could affect the behavior of the slugs.

1 Introduction

Slug flow is an intermittent two-phase flow regime observed when gas and liquid flow simultaneously in a pipe characterized by the alternated passage of long gas bubbles and aerated liquid slugs. This flow pattern has been continuously studied over the years due to its predominance in many industrial applications and its complexity related to an inherently unsteady characteristic. The slug flow is not always desired since its intermittent behavior allows the flow rates to oscillate which causes vibrations and higher pressure drop along the line increasing the chance of damaging the pipe supports. The flow is associated with operational problems, such as pipe fatigue occurring in turns and bends (Garcia et al., 2023, [1]), and erosion-corrosion enhancement. During slug flow, knowledge of the slug parameters is important for the design of production facilities, and the calculation of pressure drop and slug length. For instance, according to Al-Safran et al. (2005) [2], the maximum slug length is the most crucial flow characteristic for proper separator or slug-catcher design.

* Corresponding author: korelstein@truboprovod.ru

The complexity of this type of flow motivated the development of mathematical models that were somehow able to describe the physical behavior behind this phenomenon. The unit cell model is a mechanistic approach derived from the mass and momentum balances coupled with empirical correlations. The unit cell model can predict the hydrodynamics of the flow based on a simplified but accurate way. According to Fagundes Netto *et al.* (2019) [3], the unit cell model estimates the average slug flow parameters by approximating the transient, chaotic phenomenon through a steady periodic structure that is repeated downstream. The concept of the model, originally proposed by Dukler and Hubbard (1975) [4], treats the slug as a unit cell, in which the control volume encompasses a liquid slug and a long gas bubble that moves in a moving frame of reference. Then, the derived mass and momentum equations are conserved at the interface between the gas and liquid phases. Additionally, the size and frequency of slug bodies show variations that could be represented in statistical distributions.

The generation of slugs from an equilibrium level could be explained by the wave growth due to the Kelvin-Helmoltz instability, with the existence of gravity force, and suction force. After slug initiation and once slugs have developed, the statistical analysis shows that the slug length is best represented by the log-normal distribution (Woods et al., 2006, [5]). The lognormal probability density function of a property or variable ($\xi > 0$) is defined as follows

$$P(\xi) = \frac{1}{\xi\sqrt{2\pi}\sigma_{LN}} e^{\left(-\frac{(ln(\xi)-\mu)^2}{2\sigma_{LN}^2}\right)}, \quad (1)$$

where μ is average, and σ_{LN} is the standard deviation of the normally transformed distribution. According to Ujang et al. (2006) [6], the standard deviation of the variable's natural logarithm (σ_{LN}) was oscillating from 0.3 to 0.8 for slug length distributions based on experiments of initiation and evolution of slugs in a 37 m horizontal pipe 0.078 m ID with air and water. Al-Safran et al. (2005) [2] found that a log-normal probability model is an appropriate model for slug-length distribution in horizontal pipelines. Two empirical relationships for mean slug length and slug-length standard deviation were developed, including the normalized momentum-exchange rate between the liquid film and the slug body (Θ). Thus, for the slug-length standard deviation, the experimental data gives the following regression model

$$\sigma_{LN} = 0.297 - 1.027H_f + 0.995\Theta, \quad (2)$$

$$\Theta = \frac{H_f(v_m - v_f)(v_T - v_f)}{v_m^2}, \quad (3)$$

where H_f is film liquid holdup, v_m is mixture velocity, v_T is translational velocity, and v_f is film velocity. Later, Al-Safran et al. (2013) [7] conclude that the slug-length distribution under high-viscosity-liquid conditions is truncated and right-skewed, deviating from the lognormal distribution of low-viscosity conditions. Similarly, for slug frequency, there are many factors contributing to randomness as the existence of different slug initiation mechanisms such as wave growth and wave coalescence (Al-Safran, 2016) [8]. Slug initiation may be reasonably approximated as an uncorrelated Poisson process with an exponential distribution (Ujang et al., 2006) [6], and the slug frequency randomness has been proposed to be modeled using the same approach (Al-Safran, 2016) [8].

The stochastic character of the slug flow can have a special application for pipe stress analysis, thus, it is included to estimate the force on pipe bends, for example in the work of Klinkenberg and Tijsseling (2021) [9]. In this study, the authors combined the unit slug model, the lognormal probability distribution for slug length, and the momentum balance

around the pipe bend, and assumed that the film and the slug are discrete to model the force spectrum.

The present work aims at investigating the stochastic nature of two-phase horizontal slug flow under different flow conditions. To achieve this objective, an experimental study was conducted, in which slug characteristics data of several slug units (l_U) with a wide range of liquid and gas superficial velocities (v_{SL} 0.2-2.0 m/s, v_{SG} 0.8-4.2 m/s) for oil-air flow were acquired. The average, and the standard deviation of the normally transformed distribution for slug length (l_s), film length (l_f), film region fraction (l_f/l_U), and slug frequency (f_s) were obtained for 30 slug flow conditions. In addition, a study based on each slug unit observed in the experimental campaign is carried out to investigate the stochastic behavior of this flow pattern through the relation between slug and film lengths.

2 Experimental program

This section describes the experimental facility and the instrumentation used for the slug measurements. This experimental facility allowed the investigation of slug length, film length, frequency, and structure velocities across a broad range of liquid and gas superficial velocities.

2.1 Slug characterization loop

For the present study, the 50.8-mm (2-in) ID horizontal oil/gas two-phase experimental flow loop of the Tulsa University Fluid Flow Projects (TUFFP) is used. The facility schematic is detailed in Figure 1. This facility has an oil transfer tank, progressive cavity pump (20-hp screw pump), oil heater (20-kW Chromalox, 21-60°C), gas (air) delivering system (20-hp Gardner Denver dry rotary screw-type compressor, 1030 CFM at 100 psig), Y-2 type liquid/gas mixing tee (gas flows through thin pipes to avoid the formation of premature slugs), and 18.9-m long clear PVC horizontal pipe. The instrumentation includes Micro-Motion mass flow meters, capacitance probes (CP, two-wire type), resistance temperature detectors, pressure transducers, and differential pressure sensors. One pair of CP (CP1 and CP2) is used to analyze the slug characteristics, such as the slug length and frequency, and translational velocity.

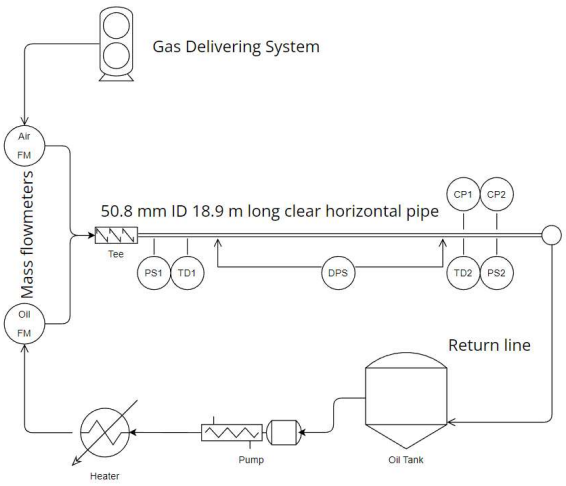

Fig. 1. Schematic of the experimental facility (TUFFP).

2.2 Capacitance sensors

Two capacitance sensors, based on the dielectric constants of air and oil, are installed at the test section to measure in-situ liquid holdup and the velocity of flow structures. The sensors have been calibrated using the procedure proposed by Brito (2012) [10]. A calibration curve is built using a set of quick-closing valves. The calibration curve is utilized to convert dimensionless voltages into liquid holdup values (H_L).

Figure 2a illustrates how a slug unit is converted from a capacitance sensor voltage to a vector of zeros and ones, defining a threshold value to characterize film and slug regions. Figure 2b presents the probability density histogram of dimensionless voltage values obtained by the CPs. In this histogram, the region where V' is low and the frequency is high is defined as the film region. The region in which both V' and the frequency are high is defined as the slug body. Between these two regions, a region with a low frequency and uniform distribution can be detected. It represents the range of possible threshold values to distinguish the film from the slug regions. Thus, the size of these structures could be obtained including the measurement of translational velocity.

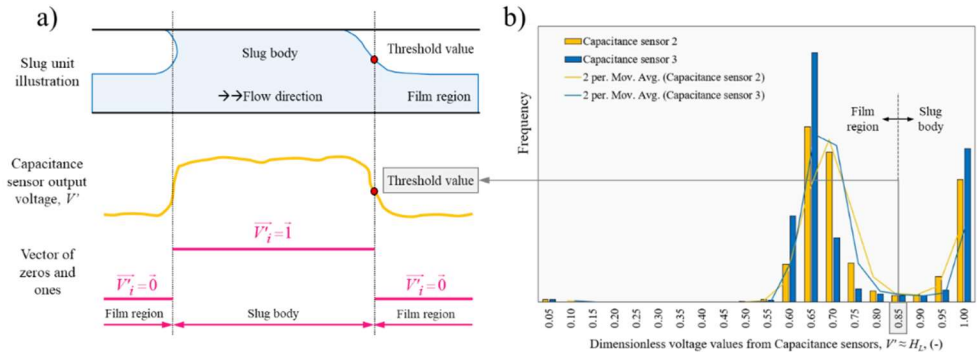

Fig. 2. (a) Separation of slug body and film region, (b) Probability density histogram of the dimensionless voltage of CPs to select a threshold value.

2.3 Instrumentation and data acquisition system

During the experiments, a data acquisition system monitors pressure, temperature, output voltage from capacitance sensors, and gas and liquid mass flow rates. This system consists of a PC, a multifunction I/O board, and the LabVIEW™ software package. All of the data files have TDMS format with a total test time of at least 1 minute. The high-speed data acquisition system has a rate of 1000 samples per second. Instrument systematic uncertainties are included for flow rates, densities, temperature, and pressure.

2.4 Fluid and operational conditions

Low-viscosity mineral oil was used during the experiments as the liquid phase. The oil has a light yellow color, and its viscosity and density were characterized using a dynamic rheometer and single-phase oil runs in the facility and are presented in Table 1 for the temperature at 80 °F. A wide range of liquid and gas superficial velocities were studied (v_{SL} 0.2-2.0 m/s, v_{SG} 0.8-4.2 m/s).

Table 1. Properties of mineral oil.

Viscosity, μ_L (cp)	Density, ρ_L (kg/m^3)	Surface tension, σ (N/m)	Color
6.2 @ 80 °F	798 @ 80 °F	0.023	Light yellow

3 Experimental results

The characterization of flow structures such as slug body or film regions and frequencies is performed by monitoring the in-situ liquid holdup (H_L), with the capacitance probes. Using dimensionless voltage tracking, it is possible to isolate the slug structures by characterizing the size of slug bodies, film regions, and the values of slug frequencies. Figures 3 show an example and its corresponding no-slip void fraction ($v_{SG}/(v_{SL}+v_{SG})$). These graphs show the capacitance probe signal response over time, revealing the fluid structures that are encountered.

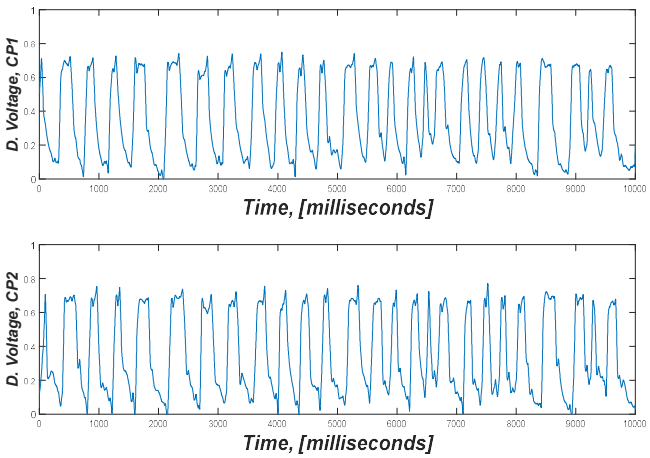

Fig. 3. Slug flow characterization ($v_{SL} = 1.60\ m/s, v_{SG} = 1.66\ m/s$, void fraction 0.51).

Table 2 shows 30 different slug flow conditions that were herein evaluated (superficial liquid velocity, v_{sL}; superficial gas velocities, v_{sG} ; mixture velocity, v_m; no-slip void fraction; and translational velocity, v_T), and the total number of slugs (slug units) encountered in the experimental test and used for the analysis.

Table 2. Flow Conditions.

#	*V*sL [m/s]	VsG [m/s]	Slug Units	Vm [m/s]	Void Frac.	Vt [m/s]	#	VsL [m/s]	VsG [m/s]	Slug Units	Vm [m/s]	Void Frac.	Vt [m/s]
1	0.20	1.04	26	1.24	0.84	1.77	**16**	1.30	1.74	84	3.04	0.57	3.99
2	0.30	1.03	40	1.34	0.77	1.96	**17**	1.29	2.51	83	3.80	0.66	4.82
3	0.41	1.02	39	1.42	0.72	2.15	**18**	1.29	3.18	77	4.47	0.71	5.68
4	0.40	1.49	39	1.89	0.79	2.78	**19**	1.60	0.89	144	2.49	0.36	3.28
5	0.50	1.02	34	1.52	0.67	2.24	**20**	1.60	1.27	130	2.87	0.44	3.76
6	0.49	1.49	31	1.98	0.75	2.87	**21**	1.60	1.66	110	3.25	0.51	4.19
7	0.49	1.93	28	2.42	0.80	3.55	**22**	1.60	2.34	113	3.94	0.60	5.01
8	0.70	1.00	66	1.70	0.59	2.43	**23**	1.59	3.04	112	4.63	0.66	5.81

9	0.70	1.45	35	2.15	0.67	3.01	**24**	1.60	3.69	107	5.29	0.70	6.55
10	0.70	1.93	32	2.63	0.73	3.65	**25**	1.60	4.19	96	5.79	0.72	7.1
11	1.01	0.95	69	1.96	0.49	2.66	**26**	1.99	0.84	192	2.83	0.30	3.76
12	1.00	1.37	62	2.38	0.58	3.19	**27**	2.00	1.20	178	3.20	0.37	4.06
13	1.00	1.81	58	2.81	0.65	3.76	**28**	2.00	1.53	181	3.53	0.44	4.41
14	1.29	0.95	109	2.24	0.42	2.94	**29**	2.00	2.20	172	4.20	0.52	5.32
15	1.29	1.32	83	2.61	0.51	3.5	**30**	1.99	2.78	160	4.78	0.58	6.09

Using EasyFit software, more than 60 probability density functions were evaluated for all the slug flow parameters. Table 3 shows the ranking of the three best functions with two parameters (2P) for each slug condition based on the experimental results. From the overall analysis of all slug characteristics, the Lognormal is the recurrent function identified as number 1 in the ranking, followed by the Gamma function which also shows a good performance. For slug length, the Lognormal distribution appeared in approximately 87% of the cases as the first one in the ranking. In the film length analysis, it appeared in 53%, and for frequency, in 30% of the cases. Other functions included in the ranking for the prediction of the stochastic nature of slug length, film length, and slug frequency are Weibull, Chi-squared (2P), Normal, and Rayleigh (2P).

Table 3. Probability density function ranking.

Cond.	**Slug Length**			**Film Length**			**Slug Frequency**		
#	**Rnk1**	**Rnk2**	**Rnk3**	**Rnk1**	**Rnk2**	**Rnk3**	**Rnk1**	**Rnk2**	**Rnk3**
1	Lognormal	Weibull	Chi-squared (2P)	Gamma	Lognormal	Weibull	Gamma	Weibull	Normal
2	Lognormal	Chi-squared (2P)	Weibull	Lognormal	Chi-squared (2P)	Rayleigh (2P)	Normal	Gamma	Weibull
3	Lognormal	Weibull	Gamma	Normal	Weibull	Gamma	Lognormal	Gamma	Rayleigh (2P)
4	Lognormal	Weibull	Chi-squared (2P)	Gamma	Chi-squared (2P)	Lognormal	Rayleigh (2P)	Lognormal	Gamma
5	Lognormal	Weibull	Chi-squared (2P)	Gamma	Lognormal	Rayleigh (2P)	Weibull	Normal	Lognormal
6	Lognormal	Chi-squared (2P)	Weibull	Lognormal	Chi-squared (2P)	Gamma	Gamma	Normal	Weibull
7	Chi-squared (2P)	Lognormal	Weibull	Lognormal	Gamma	Weibull	Lognormal	Rayleigh (2P)	Gamma
8	Lognormal	Weibull	Gamma	Lognormal	Gamma	Rayleigh (2P)	Normal	Weibull	Gamma
9	Lognormal	Weibull	Gamma	Gamma	Lognormal	Weibull	Weibull	Normal	Rayleigh (2P)
10	Lognormal	Gamma	Chi-squared (2P)	Gamma	Weibull	Lognormal	Normal	Weibull	Gamma
11	Lognormal	Gamma	Rayleigh (2P)	Lognormal	Gamma	Rayleigh (2P)	Rayleigh (2P)	Gamma	Lognormal
12	Lognormal	Weibull	Gamma	Gamma	Rayleigh (2P)	Normal	Weibull	Normal	Gamma
13	Lognormal	Gamma	Weibull	Chi-squared (2P)	Lognormal	Gamma	Weibull	Normal	Gamma
14	Lognormal	Gamma	Weibull	Lognormal	Rayleigh (2P)	Gamma	Normal	Gamma	Weibull
15	Lognormal	Gamma	Weibull	Lognormal	Gamma	Rayleigh (2P)	Gamma	Lognormal	Rayleigh (2P)
16	Lognormal	Gamma	Rayleigh (2P)	Lognormal	Gamma	Rayleigh (2P)	Rayleigh (2P)	Gamma	Lognormal
17	Lognormal	Gamma	Weibull	Normal	Gamma	Weibull	Gamma	Lognormal	Weibull
18	Weibull	Lognormal	Rayleigh (2P)	Gamma	Normal	Lognormal	Normal	Rayleigh (2P)	Gamma
19	Lognormal	Gamma	Rayleigh (2P)	Rayleigh (2P)	Gamma	Lognormal	Lognormal	Gamma	Normal
20	Lognormal	Gamma	Weibull	Lognormal	Rayleigh (2P)	Gamma	Gamma	Lognormal	Normal

21	Lognormal	Rayleigh (2P)	Weibull	Lognormal	Gamma	Rayleigh (2P)	Lognormal	Gamma	Normal
22	Lognormal	Gamma	Rayleigh (2P)	Lognormal	Gamma	Rayleigh (2P)	Rayleigh (2P)	Lognormal	Gamma
23	Lognormal	Gamma	Weibull	Normal	Weibull	Gamma	Lognormal	Gamma	Rayleigh (2P)
24	Gamma	Lognormal	Weibull	Lognormal	Gamma	Weibull	Lognormal	Gamma	Rayleigh (2P)
25	Lognormal	Weibull	Rayleigh (2P)	Gamma	Lognormal	Normal	Lognormal	Gamma	Rayleigh (2P)
26	Rayleigh (2P)	Gamma	Lognormal	Lognormal	Rayleigh (2P)	Gamma	Rayleigh (2P)	Lognormal	Gamma
27	Lognormal	Gamma	Rayleigh (2P)	Lognormal	Gamma	Rayleigh (2P)	Gamma	Normal	Lognormal
28	Lognormal	Rayleigh (2P)	Gamma	Lognormal	Gamma	Rayleigh (2P)	Lognormal	Gamma	Normal
29	Lognormal	Gamma	Rayleigh (2P)	Lognormal	Gamma	Rayleigh (2P)	Lognormal	Gamma	Normal
30	Lognormal	Gamma	Rayleigh (2P)	Gamma	Lognormal	Rayleigh (2P)	Gamma	Normal	Lognormal

This study suggested the appropriateness of a lognormal model for representing slug characteristics distribution, such as slug length, film length, and frequency. Therefore, Table 4 includes the parameters of the lognormal function for slug length [ft], film length [ft], film region fraction [-], and slug frequency [s-1] that were obtained and best fitted the experimental data.

Table 4. Lognormal probability function for slug flow parameters.

Cond.	**Slug Length, [ft]**			**Film Length, [ft]**			**Film Region Fraction, [-]**			**Slug Frequency, [s-1]**		
#	**μ**	**σLN**	**Mean**	**μ**	**σLN**	**Mean**	**μ**	**σLN**	**Mean**	**μ**	**σLN**	**Mean**
1	1.37	0.59	4.7	3.69	0.31	42.0	-0.12	0.13	0.89	-2.03	0.28	0.14
2	1.40	0.59	4.8	3.16	0.24	24.3	-0.18	0.11	0.84	-1.46	0.24	0.24
3	1.29	0.53	4.2	2.76	0.28	16.4	-0.23	0.13	0.80	-1.04	0.28	0.37
4	1.31	0.57	4.4	3.13	0.29	23.9	-0.18	0.12	0.84	-1.10	0.28	0.35
5	1.12	0.52	3.5	2.37	0.24	11.0	-0.27	0.14	0.77	-0.65	0.27	0.54
6	1.30	0.65	4.5	2.86	0.30	18.3	-0.22	0.13	0.81	-0.84	0.30	0.45
7	1.32	0.70	4.8	3.19	0.35	25.8	-0.17	0.13	0.85	-0.90	0.36	0.43
8	1.08	0.49	3.3	1.98	0.25	7.5	-0.37	0.19	0.70	-0.28	0.23	0.78
9	1.13	0.59	3.7	2.39	0.33	11.5	-0.26	0.13	0.78	-0.35	0.32	0.74
10	1.26	0.52	4.0	2.78	0.31	16.9	-0.23	0.17	0.81	-0.54	0.23	0.60
11	0.90	0.44	2.7	1.37	0.24	4.1	-0.51	0.20	0.61	0.29	0.22	1.37
12	1.03	0.47	3.1	1.82	0.29	6.4	-0.41	0.21	0.68	0.12	0.24	1.16
13	1.11	0.48	3.4	2.17	0.23	9.0	-0.32	0.15	0.73	0.02	0.23	1.05
14	0.72	0.43	2.3	0.95	0.25	2.7	-0.61	0.22	0.56	0.70	0.25	2.08
15	0.97	0.46	2.9	1.45	0.33	4.5	-0.52	0.24	0.61	0.47	0.26	1.65
16	0.95	0.52	3.0	1.68	0.24	5.5	-0.43	0.19	0.66	0.46	0.24	1.63
17	1.08	0.47	3.3	2.00	0.28	7.7	-0.36	0.19	0.71	0.39	0.24	1.52
18	1.18	0.51	3.7	2.29	0.30	10.3	-0.31	0.16	0.74	0.32	0.27	1.43
19	0.69	0.35	2.1	0.56	0.26	1.8	-0.78	0.23	0.47	1.04	0.23	2.91
20	0.81	0.41	2.4	1.02	0.26	2.9	-0.62	0.22	0.55	0.87	0.25	2.46
21	0.93	0.45	2.8	1.31	0.27	3.8	-0.55	0.21	0.59	0.77	0.28	2.25
22	0.97	0.48	3.0	1.56	0.28	4.9	-0.47	0.21	0.64	0.77	0.27	2.24
23	1.05	0.46	3.2	1.82	0.32	6.5	-0.42	0.20	0.67	0.71	0.27	2.11
24	1.15	0.50	3.6	2.01	0.38	8.0	-0.39	0.22	0.69	0.66	0.31	2.03
25	1.10	0.49	3.4	2.13	0.32	8.9	-0.33	0.15	0.73	0.68	0.29	2.06
26	0.70	0.37	2.2	0.14	0.29	1.2	-1.04	0.28	0.37	1.34	0.28	3.97
27	0.73	0.34	2.2	0.46	0.30	1.7	-0.86	0.23	0.43	1.27	0.25	3.67

28	0.74	0.38	2.3	0.70	0.26	2.1	-0.74	0.24	0.49	1.24	0.25	3.57
29	0.82	0.40	2.5	1.07	0.28	3.0	-0.60	0.20	0.56	1.19	0.27	3.41
30	0.97	0.42	2.9	1.34	0.26	4.0	-0.56	0.20	0.58	1.10	0.24	3.09

Figure 4 shows the statistical distributions of the slug structures for the same condition as presented in Figure 3. In Figure 4, the mean values of the distributions are also presented, together with the lognormal parameters. The mean value from the probability function is calculated as follows

$$Mean(\xi) = e^{\left(\mu + \frac{\sigma_{LN}^2}{2}\right)}. \quad (4)$$

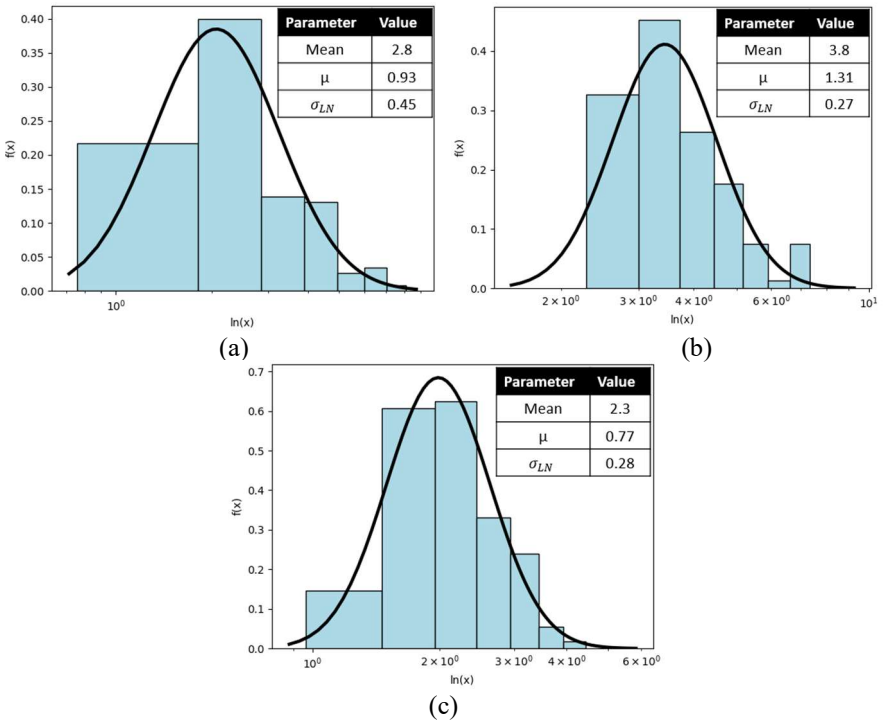

Fig. 4. Log-normal probability density function in semi-log scale (Slug flow, $v_{SL} = 1.60\ m/s, v_{SG} = 1.66\ m/s$) for: a) slug length [ft], b) film length [ft], and c) slug frequency [s-1]. Flow condition case #21.

From the presented results, it is possible to observe that the lognormal distribution shows an acceptable fit to the overall data.

Figure 5 presents the relationship between the void fraction and the standard deviations for all the slug flow parameters. The standard deviation for slug length varies from 0.4 to 0.7 depending on gas (void) fraction, which is in agreement with the commonly used value of 0.5 to determine extreme sizes (Brill et al., 1981) [11]. In addition, the standard deviations for film length and slug frequency are practically the same and have a constant behavior of around 0.3. The slug length shows a wider range of values once the void fraction increases. This could be related to the proximity to the high gas conditions more related to pseudo-slug (PSL) flow and annular flow.

A flow pattern map was generated based on the fluid properties and pipe geometry of this study using Barnea's model for predicting flow-pattern transitions (Barnea, 1987) [12]. The

experimental test matrix is presented in Figure 6 with the operational points and the transitions to different flow patterns. The transition to pseudo-slug flow was obtained based on experimental measurements and observations. Thus, as the gas flow rate further increases, the flow pattern changes from slug (SL) to pseudo-slug (PSL), which is identified due to a continuous gas passage through the slug bodies and is characterized by high variations in the size and density of flow structures (Soedarmo, 2018) [11].

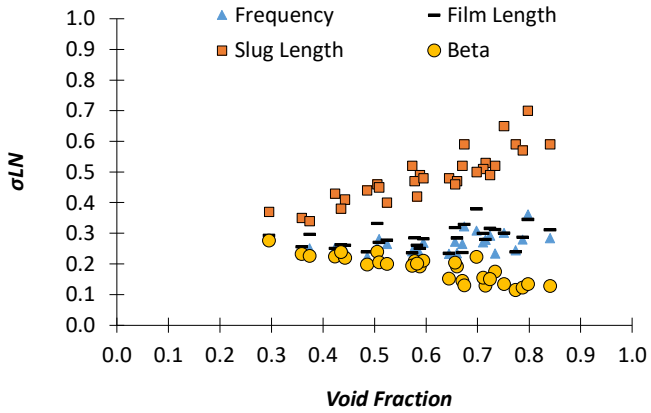

Fig. 5. Standard deviation of the normally transformed distribution (σ_{LN}). Experimental analysis.

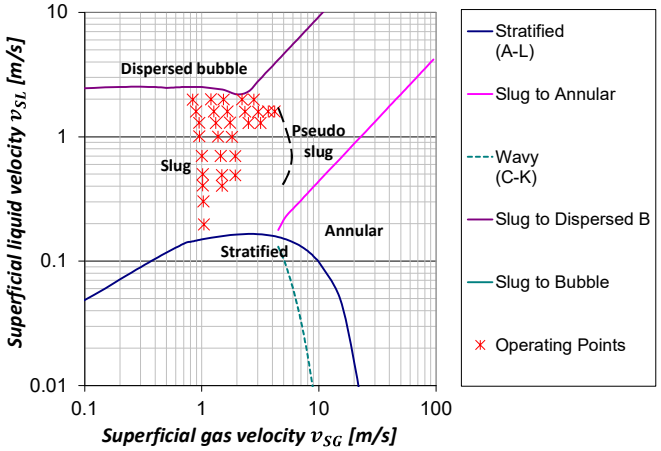

Fig. 6. Experimentally observed flow pattern on top of Barnea's (1987) map.

In Figure 7, the mean values of the slug flow parameters (slug length, film length, film length ratio, and frequency) are compared against the gas fraction. In the graph, the film length ratio is addressed as beta. Based on the mean results presented in Figure 7, slug length and film length tend to increase as more gas is present in the flow. The trend of the mean frequency indicated that higher frequencies are expected when lower gas fractions are obtained. Frequency and film length have opposite behaviors, which means that higher frequencies are expected for lower film lengths, as is observed for slug flow conditions that approach the dispersed bubble flow pattern. The film length ratio is mostly affected by the film length, so it tends to increase once the film length increases.

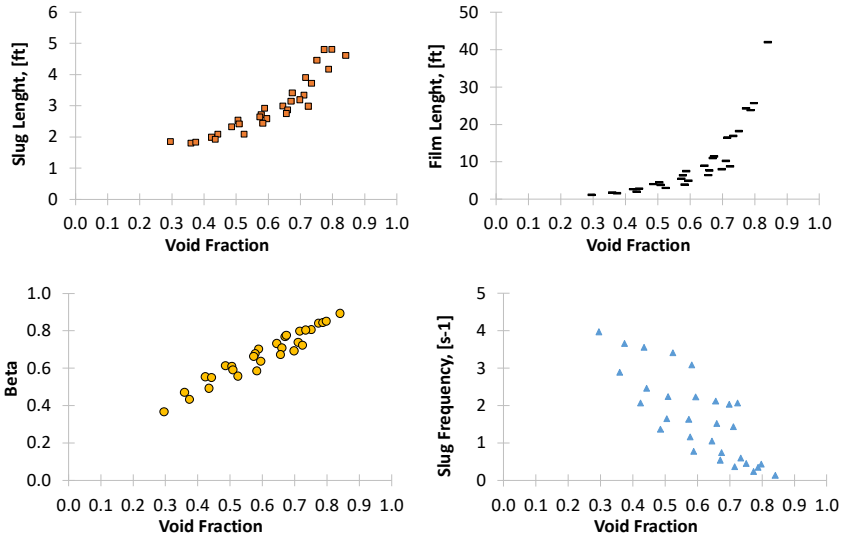

Fig. 7. Change of slug flow characteristics influenced by the gas fraction (mean values).

Trends in the mean slug flow parameters can be identified, as presented in the previous graphs. Once the train of slugs is analyzed, the hydrodynamic behavior is more complex due to the intrinsic intermittency of each slug unit. In this study, three different approaches to analyze the data were used: slug unit starting from a slug body followed by a film region; slug unit starting from a film region followed by a slug body; and slug unit composed by a slug body and the average of two film regions (one before and one after the slug body). Figure 8 shows the schematic for each approach.

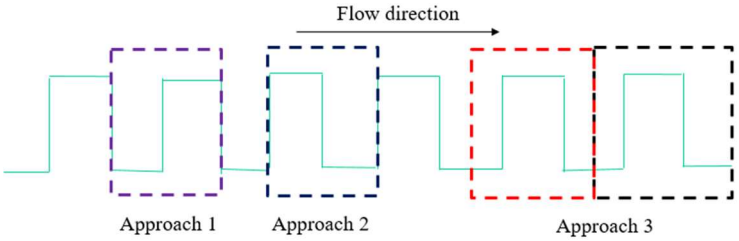

Fig. 8. Schematic of different approaches to analyzing the data.

Each approach was implemented to verify the relation between slug and film lengths. The results with approach 1 did not show a direct relation between slug and film lengths when all slug units in the experimental test were analyzed. Approaches 2 and 3 presented similar results to each other, however in an overall investigation of the slug flow conditions, approach 2 was able to reveal a clear relation between the lengths, therefore approach 2 is the one used in the further analysis. In addition, slug flow conditions in a region close to the stratified flow (operational points at the bottom of the map in Fig. 6) did not show a clear relation, in terms of the coefficient of determination (R-squared, R^2), in all the approaches studied. This can be observed in Figure 9, where the R^2 obtained for the relation between slug length and film length is plotted in the flow pattern map. This might be associated with the lower number of slug units observed in the period that the experimental data was acquired

due to their lower slug frequency, affecting the uncertainties of the analysis for these conditions.

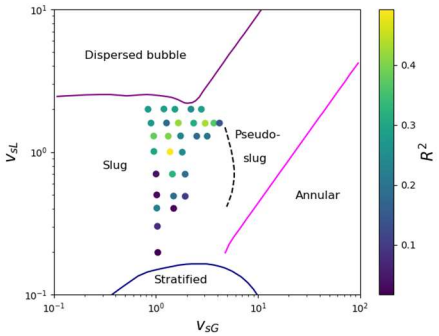

Fig. 9. Coefficient of determination obtained from the relation between the slug and film lengths in terms of the superficial liquid and gas velocities for all the conditions.

The following graphs in Figure 10 show a comparison of film length vs slug length, beta (film length ratio) vs slug length, unit length vs slug length, and unit length vs film length for all the slug units observed in each test. The flow conditions correspond to different void fractions, cases #6 (blue markers), #23 (red markers), and #26 (yellow markers) in Table 3, showing a detailed study comparing the characteristics of each slug unit.

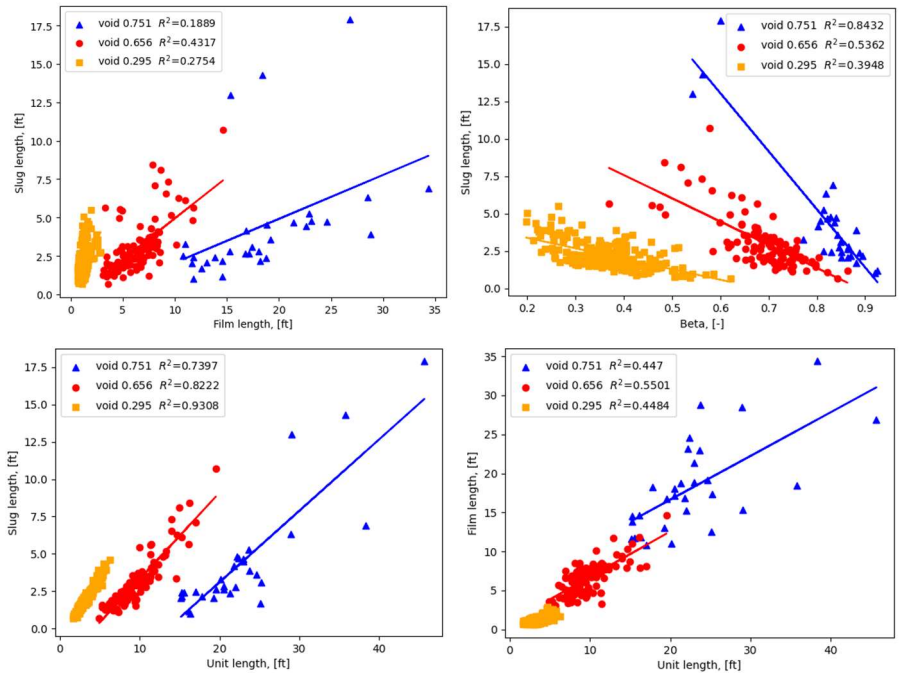

Fig. 10. (a) Relation between film length vs slug length (left top), (b) beta vs slug length (top right), (c) unit length vs slug length (left bottom), and (d) unit length vs film length (right bottom) for different slug flow structures.

In Figure 10, the coefficient of determination (R-squared, R^2) is presented in the legend of each figure for each slug flow condition. It can be observed in Fig. 10 (a), that the results

suggest a relation between slug and film lengths, even though this relation is more clear for some slug flow conditions than for others. The inclinations of the curves in Fig. 10 (a) are higher once the film length ratio (beta) is smaller. It is possible to notice from Fig. 10 (b) that beta is generally smaller for the case with a lower void fraction. The relationships between unit length and slug and film lengths, Figs. 10 (c) and (d) respectively, show a linear trend.

The R^2 (below 0.5) values for the relation between slug length and film length can be an indication of the influence of other flow parameters that also have stochastic nature, such as slug liquid holdup, that could affect the behavior of each slug unit. Within the same flow condition, each slug unit may have changes in the dynamics while traveling along the line.

For future analysis, it is recommended a deeper study for each slug considering the variation not only in lengths but also in flow characteristics such as slug and film holdups, and aeration in the slug body. Another suggestion would be to increase the sampling time for low slug frequency conditions, in lower superficial liquid velocities, to analyze more slug units. A systematic way to remove the outliers from the data is also a further recommendation from this work.

4 Conclusion

In the present work, an experimental campaign with 30 slug flow conditions (v_{SL} 0.2-2.0 m/s, v_{SG} 0.8-4.2 m/s) in a horizontal 2-in ID pipe with oil and air was carried out. Based on the experimental statistical analysis, it was identified that the lognormal distribution shows an appropriate representation of the slug characteristics, such as slug length, film length, and frequency. Based on the trend of the mean values, slug length, and film length tend to increase as more gas is present in the flow, while frequency increases with lower lengths.

In addition, the entire distribution of slugs was analyzed individually and it shows more complex behavior because of the intrinsic randomness of the slug flow. For this study, three different approaches to analyze the data were used and the results show that the slug and film lengths suggest a relation when the slug unit is characterized by the film region followed by the slug body region. The R^2 values (below 0.5) characterizing the relationship between slug length and film length may indicate that other flow parameters with stochastic nature such as slug liquid holdup, could impact the behavior of each slug unit.

References

1. C. Garcia, R. Nemoto, E. Pereyra, L. Korelstein, C. Sarica, International Journal of Multiphase Flow, 104321, **159** (2023)
2. E. M. Al-Safran, C. Sarica, H. Q. Zhang, J. P. Brill, *SPE Production and Facilities*, 84230 (2005)
3. J. R. Fagundes Netto, G. F. N. Gonçalves, A. P. Silva Freire, International Journal of Multiphase Flow, 10.086, **120** (2019)
4. E. Dukler, M. G. Hubbard, Ind. Eng. Chem. Fundam., 377-347, **14**, 4 (1975)
5. B. D. Woods, Z. Fan, T. J. Hanratty, International Journal of Multiphase Flow, 902-925, **32** (2006)
6. P. M. Ujang, C. J. Lawrence, C. P. Hale, G. F. Hewitt, International Journal of Multiphase Flow, 527-552, **32** (2006)
7. E. M. Al-Safran, B. Gokcal, C. Sarica, *SPE Production and Facilities*, 150572 (2013)
8. E. M. Al-Safran, Journal of Petroleum Science and Engineering, 88-96, **138** (2016)

9. A. M. Klinkenberg, A. S. Tijsseling, International Journal of Multiphase Flow, 103778, **144** (2021)
10. R. Brito, University of Tulsa, Master of Science thesis, **119** (2012)
11. J.P. Brill, Z. Schmidt, W.A. Coberly, J.D. Herring, D.W. Moore, Society of Petroleum Engineers Journal, 363-378 (1981)
12. D. Barnea, International Journal of Multiphase Flow, 1-12, **13** (1987)
13. A. Soedarmo, E. Pereyra, C. Sarica, Offshore Technology Conference, 28996, (2018)